Article

A Probabilistic Ensemble Prediction Method for PV Power in the Nonstationary Period

Yuan An, Kaikai Dang, Xiaoyu Shi *, Rong Jia, Kai Zhang and Qiang Huang

College of Electrical Engineering, Xi'an University of Technology, Xi'an 710048, China;
yy19820316@163.com (Y.A.); dangkaii@sina.cn (K.D.); jiarong@xaut.edu.cn (R.J.);
2180421165@stu.xaut.edu.cn (K.Z.); sy-sj@xaut.edu.cn (Q.H.)
* Correspondence: sxy_xaut@126.com

Abstract: Due to the large number of grid connection of distributed power supply, the existing scheduling methods can not meet the demand gradually. The proposed virtual power plant provides a new idea to solve this problem. The photovoltaic power prediction provides the data basis for the scheduling of the virtual power plant. Prediction intervals of photovoltaic power is a powerful statistical tool used for quantifying the uncertainty of photovoltaic power generation in power systems. To improve the interval prediction accuracy during the non-stationary periods of photovoltaic power, this paper proposes a probabilistic ensemble prediction model, which combines the modules of data preprocessing, non-stationary period discrimination, feature extraction, deterministic prediction, uncertainty prediction, and optimization integration into a general framework. More specifically, in the non-stationary period discrimination module, the method of discriminating the difference of the power ratio difference is introduced and applied for identifying the non-stationary period of the data of photovoltaic output; in the deterministic point prediction module, a stacking- long-short-term memory neural network model is used for point forecasts; in the uncertainty interval prediction module, a BAYES neural network is introduced for probabilistic forecasts; in the optimization integration module, an optimization algorithm named Non-dominated Sorting Genetic Algorithm-II is applied for integrating and optimizing the results of the point forecast and probabilistic forecast. The proposed model is tested using two photovoltaic outputs and weather data measured from a grid-connected photovoltaic system. The results show that the proposed model outperforms conventional forecast methods to predict short-term photovoltaic power outputs and associated uncertainties. The interval width is reduced by 10–20%, and the prediction accuracy is improved by at least 10%; this can be a useful tool for photovoltaic power forecasting.

Keywords: multi-objective optimization; photovoltaic power; point prediction; interval prediction; ensemble probability prediction (MLBN) model

1. Introduction

In recent years, the fossil energy crisis has gradually attracted the attention of various countries, and the development momentum of new energy has been risen rapidly [1,2]. As an important part of the new energy industry, photovoltaic power generation has greatly increased its installed capacity in recent years, occupying a large share of the power system [3,4]. At the same time, photovoltaic power generation has the characteristics of randomness, volatility and intermittent. For power systems, when large-scale photovoltaic power generation systems are integrated into the main grid, they will have a great impact on the economic operation and stability of the grid, thus increasing the difficulty of power system dispatch [5,6]. On the other hand, as a solution to maximize the profit of all participants [7], virtual power plant (VPP) is the use of advanced communications and computing technology of whole organic regulation multi-type controlled source unit loads and stores, such as to reduce the effect of the randomness and volatility in the distributed

generation operation of the main network, make it an active part in power demand side management [8]. It excavates and utilizes the flexible adjustment ability of all kinds of distributed resources, which can reduce the energy cost of users and greatly promote the consumption of new energy. At present, the virtual power plant technology at home and abroad is mainly applied to the control and scheduling problem of multiple energy complementary systems [9]. In terms of traditional energy output, it can change the system output in time with the change of scheduling strategy [10]. In terms of new energy, due to the intermittent and random nature of wind and light energy, the output of the system cannot timely and effectively follow the change of scheduling strategy [11], which lays hidden risks for large-scale system scheduling. In order to solve this problem, photovoltaic power prediction arises at the historic moment. Combined with the above, it can be seen that accurate photovoltaic power prediction plays an important role in the overall regulation of virtual power plant [12]. Therefore, the prediction of photovoltaic power is of great significance for large-scale photovoltaic grid-connected power generation, improving the safety and stability of power system operation, and ensuring the safe dispatch of power grids.

The forecasting of photovoltaic power is not an easy task because PV power is affected by many factors, including irradiance, temperature, etc [13]. Under such circumstances, at present, the PV power forecasting is mainly divided into two categories according to the different prediction results: certain point/ deterministic prediction [14] and uncertainty interval prediction [15]. In recent years, many authors have focused on the research of deterministic prediction, and the method of artificial intelligence is used widely. The method digs out the relationship between the input variables implicit in the historical output data of photovoltaic power plants and the predicted results by machine learning, to realize the prediction of photovoltaic power. Common artificial intelligence algorithms mainly include BP neural network, support vector machine, regression tree algorithm, and so on [16]. Compared with the deterministic point prediction, there are fewer scholars studying the uncertainty interval prediction. Considering that photovoltaic power generation is greatly affected by meteorological factors when the meteorological conditions within the forecast period fluctuate greatly, the photovoltaic output curve will no longer be smooth, and there will be a large peak-valley difference, with the accuracy of the deterministic prediction results greatly reduced [5]. For this reason, interval forecasts can make up for the lack of deterministic forecasts and have more comprehensive information. This not only allows decision-makers to understand the possible output of the prediction point, but also helps decision-makers understand the future change trend of the output of the prediction point, thereby greatly improving the prediction accuracy, and promoting grid planning, risk analysis, and reliability evaluation [6]. Therefore, interval prediction is an advantageous tool with which to improve the accuracy of photovoltaic power prediction.

In the field of deterministic prediction, Reference [17] divides weather conditions into ideal weather and non-ideal weather types. For ideal weather, a long-short-term memory neural network (LSTM) prediction method is used; for non-ideal weather, time-series correlation and characteristics of non-ideal weather types are considered in LSTM to generate the final point prediction value. In reference to the limitations and incompleteness of photovoltaic historical output data and meteorological data, Reference [18] proposed a day-ahead prediction method similar to cloud space fusion based on this, so as to complete point prediction. Additionally, Reference [19] established an independent day-ahead PV power prediction model based on a long-short-term recurrent neural network (LSTM-RNN), and proposed a method to modify the prediction results of LSTM-RNN model based on the principle of time correlation, which improves the prediction accuracy of the model.

In the field of uncertainty prediction, Reference [4] proposed an integrated method of short-term PV power prediction based on extreme learning machine (ELM) and lower and upper bound estimation (LUBE), and used an improved differential evolution algorithm to find the best generating prediction intervals. Reference [20] proposed a new two-stage

model to quantify the prediction interval value of photovoltaic power output, integrated a variety of neural network models to generate point prediction values, and generated the prediction interval through the kernel density estimation method. Reference [21] proposed an improved Bootstrap method to improve the traditional theoretical method, solve the problem of invalid prediction error hypothesis, and reduce the interval width under the premise of ensuring interval coverage. Reference Additionally, [22] proposed a prediction model based on particle swarm optimization and boundary theory; by using particle swarm algorithm to optimize the output weight of boundary estimation theory, the interval prediction of photovoltaic output was realized.

To the best of our knowledge, each model has disadvantages and advantages. Therefore, none of these models can always achieve the desirable prediction results [23,24]. To further improve forecasting performance, this paper proposes a multi-objective optimization-based ensemble probability forecasting (MLBN) model for the non-stationary period of photovoltaic output based on the research of previous authors [25,26]. Modeling is divided into three stages: in the first stage, the historical output data of photovoltaic power plants are preprocessed, feature selection is performed based on the MIC theory, and the most suitable input features are selected; in the second stage, according to the feature selection results of the first stage, the features are respectively input to the improved LSTM algorithm and the BAYES neural network to obtain the initial deterministic point prediction results and the uncertainty interval prediction results; in the third stage, the initial interval prediction value is optimized to meet the narrowest interval width and the highest interval coverage, and then the initial point prediction result is optimized and estimated, and it is expanded to a new interval prediction value. Finally, the NSGA-II optimization algorithm is used to perform multi-objective optimization of the two new interval prediction values to obtain the final prediction interval.

The main contributions of this paper are demonstrated as the follows:

(1) Considering the non-stationary nature of PV power output, the differential theory based on irradiance and power's ratio is proposed to preprocess the PV historical data.
(2) The Stack-LSTM model, which based on LSTM and Stacking learning, is put forward as a new point prediction model to improve the modeling accuracy.
(3) The multi-objective calibration of ensemble probabilistic photovoltaic power forecasting model (MLBN) is proposed, which can improve prediction accuracy by a large number and help decision-makers control the changes in the power grid planning and scheduling.

The remainder of this paper is organized as the follows. Section 2 briefly describes the basic methods about DM, Stack-LSTM, BAYES and NSGA-II. Section 3 presents the framework of the proposed MLBN model and the error indicators. Section 4 is designed for data set preprocessing and forecasting results of different models. Conclusions are given in Section 5.

2. Method Introduction

In this section, we mainly introduce the ensemble probability forecasting (MLBN) model method based on multi-objective optimization, including the power ratio difference discriminant method, point prediction model, interval prediction model, NSGA-II (Non-dominated Sorting Genetic Algorithm-II) multi-objective optimization algorithm, MIC (Maximal Information Coefficient) theory, etc.

2.1. Discrimination Method for Radiation Power Ratio Difference (DM)

The output of photovoltaic power plants has the characteristics of randomness and intermittent. In ideal weather conditions such as sunny days, the output of photovoltaic power is in a stable period; The output curve shows obvious periodic changes, and is close to the normal distribution, and the fluctuation is small [27]. In other cases, the photovoltaic output is in a non-stationary period, and the output curve fluctuates randomly with the change of the weather, with greater fluctuations than in a stable period. Therefore, this

paper proposes for the first time the method of discriminating the difference in the radiation power ratio [16]. According to the fluctuation range of the photovoltaic output curve, the historical data is divided into a stable output period and a non-steady output period. The specific discrimination process is as follows [19].

(1) Photovoltaic output is greatly affected by factors such as weather and irradiance, and it has a strong periodicity. The common output curve types are stable output type and non-stable output type. Figures 1 and 2 show representative two Group data, respectively, as the specific description of these two types.
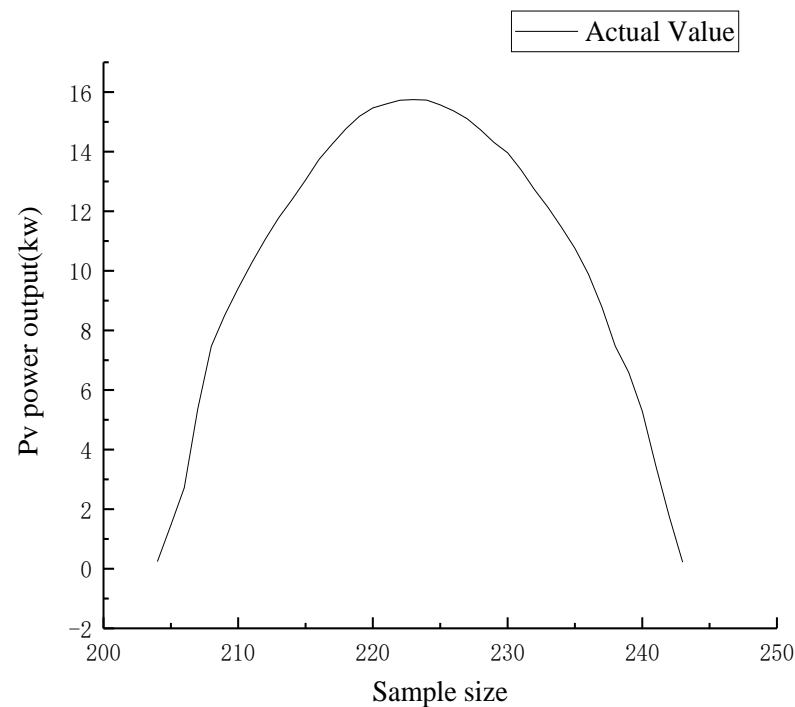

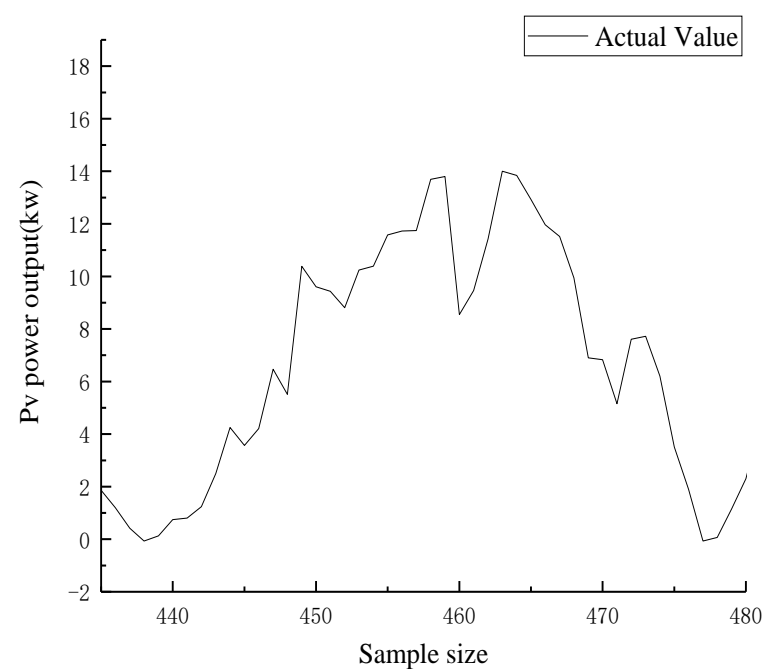**Figure 1.** Period of stable photovoltaic output.

Figure 2. Non-stationary period of photovoltaic output.

(2) In order to accurately distinguish the difference between the period of steady output and the period of non-stationary output, the steps in this paper are as follows.

(a) the parameter radiant power ratio difference can be defined as

$$X_t = \frac{S_{t-1}}{S_t} \tag{1}$$

where, S_{t-1} is the irradiance of the $(t-1)$-th sample in the data sample; S_t is the irradiance of the t-th sample in the data sample.

(b) Dividing the value range of X_t, can be expressed as

$$X_t = \left\{ \begin{array}{c} X_t < 0.7 \\ X_t > 1.3 \\ 0.7 \leq X_t \leq 1.3 \end{array} \right. \tag{2}$$

(c) The value of X_t is judged on the basis that when the value is on $[0.7, 1.3]$, which is regarded as a period of steady output, and all other cases are periods of non-steady output. Due to the large changes in power during the two periods of time when the sun rises and the sun sets for photovoltaic power generation, it is a normal phenomenon. To avoid dividing the two periods of time into non-stationary output periods in the division process, a new criterion (3) is used to prevent misjudgments.

$$|P_{t-1} - P_t| > 3 \tag{3}$$

where, P_{t-1} is the actual output power of the $(t-1)$-th sample in the data sample, and P_t is the actual output power of the t-th sample in the data sample.

After the test of this method in this paper, the radiant power ratio difference criterion method can distinguish the stable period and the non-stationary period of photovoltaic output with high quality, which has strong feasibility.

2.2. Point Prediction Model

Aiming at the characteristics of photovoltaic output during non-stationary periods, this paper adopts an improved Stack-LSTM model to predict photovoltaic power with certainty points [2,28]. The standard LSTM neural network is improved from the general recurrent neural network (RNN) recurrent neural network model, which solves the problems of long-term dependence and gradient disappearance in the RNN network; compared with other networks, the processing of nonlinear problems has greater advantages. The standard structure is shown in Figure 3.
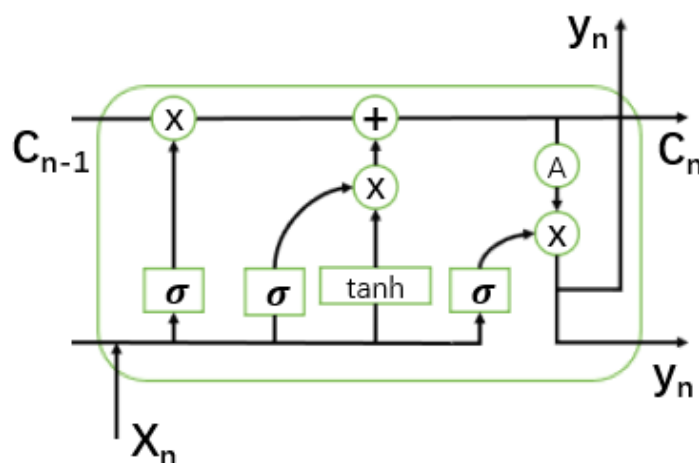

Figure 3. Schematic diagram for the standard LSTM structure.

However, in actual operation, it is found that the prediction accuracy of the standard LSTM model is not high enough for the power prediction during the non-stationary output period extracted in this paper. To further improve the prediction model and improve the prediction accuracy of non-stationary output periods, this paper introduces the integration theory based on the original LSTM model, and builds the Stack-LSTM model. The model structure diagram is shown in Figure 4, and the specific process is in the following.
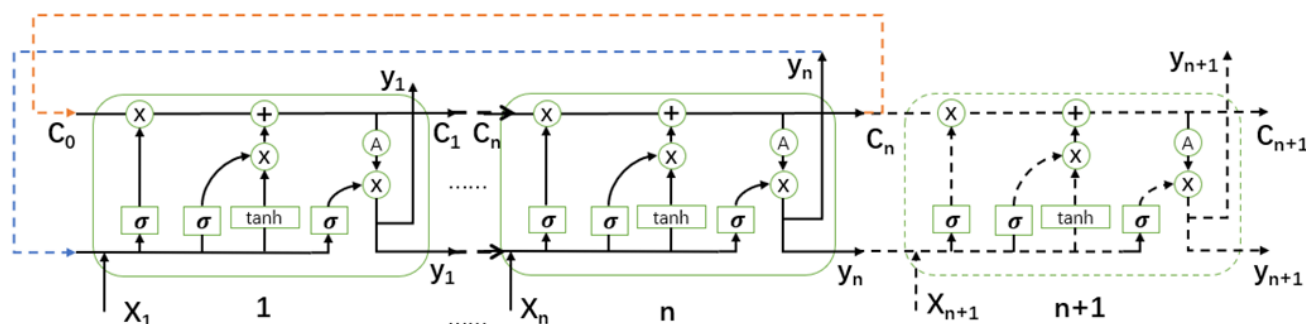

Figure 4. Stack-LSTM model structure diagram.

(1) Dividing the data set $I = \{x_i, y_i\}_{i=1}^{m}$ into n subsets $I_1, I_2, \ldots\ldots I_n$;
(2) Based on these n subsets, they are input into the LSTM algorithm to obtain the first prediction result $w_1, w_2, \ldots\ldots w_n$;
(3) The first prediction result is added as an additional feature to the original feature to form a new input feature $x'_1, x'_2, \ldots\ldots x'_l = (x_1, x_2, \ldots\ldots x_l, w_1, w_2, \ldots\ldots w_n)$, which is then input into the LSTM algorithm again to perform the second prediction and obtain a higher precision result [19].

2.3. Interval Prediction Model

Under complex weather conditions, the short-term output of photovoltaic power plants is not stable. Aiming at the problem that the prediction accuracy of the deterministic prediction method is significantly reduced, this paper uses Bayesian neural network for interval prediction [20]. Compared with deterministic forecasting, interval forecasting can give the interval distribution of all possible output values of photovoltaic equipment at the forecast time, thereby describing the uncertainty of the forecast point [1]. The Bayesian neural network is essentially a probability-based uncertainty inference network. Its structure is similar to that of a deep neural network. It is composed of an input layer, a hidden layer, and an output layer, as shown in Figure 5a. The difference is that the Bayesian neural network has a probability layer in the hidden layer of its network; the weight obeys the probability distribution and is a random variable, not a definite value [21]. The structure of the hidden layer is shown in Figure 5a,b.

In Figure 5, A and B are the input and output vectors of the hidden layer, respectively; a_n is the weight of the n-th unit, which obeys the distribution of the form $p(a_n|A, B)$, and b_n is the bias of the n-th unit [22].

The existence of the probability layer gives the Bayesian neural network the ability to describe uncertain events. Its essence is like the integrated neural network. Besides, the difference is that each sub-network of the probability layer of Bayesian neural network is not independent of each other; rather, after each training, all sub-networks can be synchronized and optimized, which makes Bayesian neural networks have a better ability to suppress the risk of overfitting than ordinary neural networks [23].
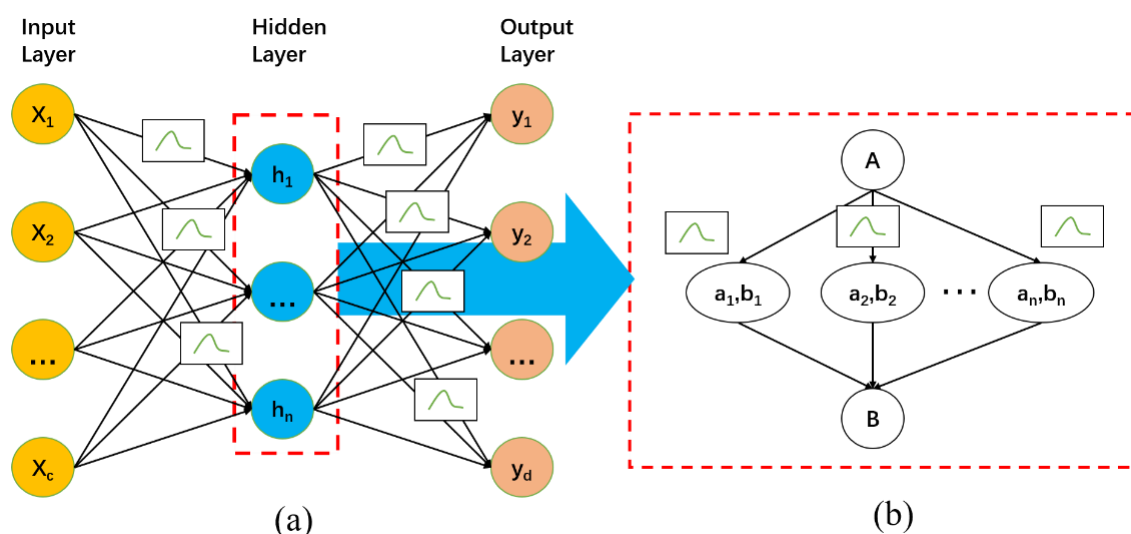
Figure 5. BAYES neural network. (**a**) BAYES neural network structure diagram; (**b**) Schematic diagram for the hidden layer of the Bayesian neural network.

2.4. Optimization of the Ensemble Prediction Model

The deterministic prediction method chooses the power value as the prediction result, which can also support the long-term optimization of the scheduling system. However, in complex weather conditions, the prediction accuracy of the deterministic point prediction is poor that would affect the safe operation of the power grid. Consequently, the probability and interval of the prediction result are unavailable. And the interval prediction method depends on the interval distribution of the photovoltaic equipment as the output to describe the uncertainty of the forecast point at the forecast point, which promotes the scheduling system to evaluate the fluctuation of output according to the predicted interval size, thereby adjusting the scheduling strategy. In addition, the interval prediction results are affected by the interval width which is restricted by the learning ability of the network. Thus, the whole prediction accuracy would be influenced by interval prediction results. Considering existed problems above, the Non-dominated Sorting Genetic Algorithm-II (NSGA-II) is introduced to conduct Multi-objective optimization about its results and improve the overall prediction accuracy [24].

The basic idea of the NSGA-II described as follows: an initial population of size N is generated randomly [25]. Then, after non-dominated sorting, the first-generation progeny population is obtained through three basic operations of the genetic algorithm including selection, crossover, and mutation; subsequently, starting from the second generation, the parent population and the offspring population are merged to perform fast non-dominated sorting [29]. Meanwhile, for forming a new parent population, the crowding degree calculation of the individuals in each non-dominated layer must be implemented according to the non-dominated relationship and the crowding degree of the individuals. Finally, a new progeny population is generated through the basic operation of the genetic algorithm; Follow above reasoning, until the conditions for the end of the program are met, the specific flowchart is shown in Figure 6.

Applying NSGA-II to the conditions described in this article, the specific process is as follows [19].

(1) Input selection. Select three points: the deterministic point prediction result, the upper and lower bounds of the interval distribution from the interval prediction, and the actual output value about this point as the input variables of the network.

(2) Model construction. By inputting the relevant variables selected above, a basic NSGA-II network model is constructed to perform multi-objective optimization. The optimization objectives are (*PINAW*) the smallest interval width and (*PICP*) the largest interval coverage. Owing to these two indicators are contradictory in the

same network, the optimization constraint must weigh them, and choose the smallest interval width under the maximum interval coverage as the restrictions.

(2) Model validation. After experiments in the subsequent part of this article, the feasibility of the model would be verified.
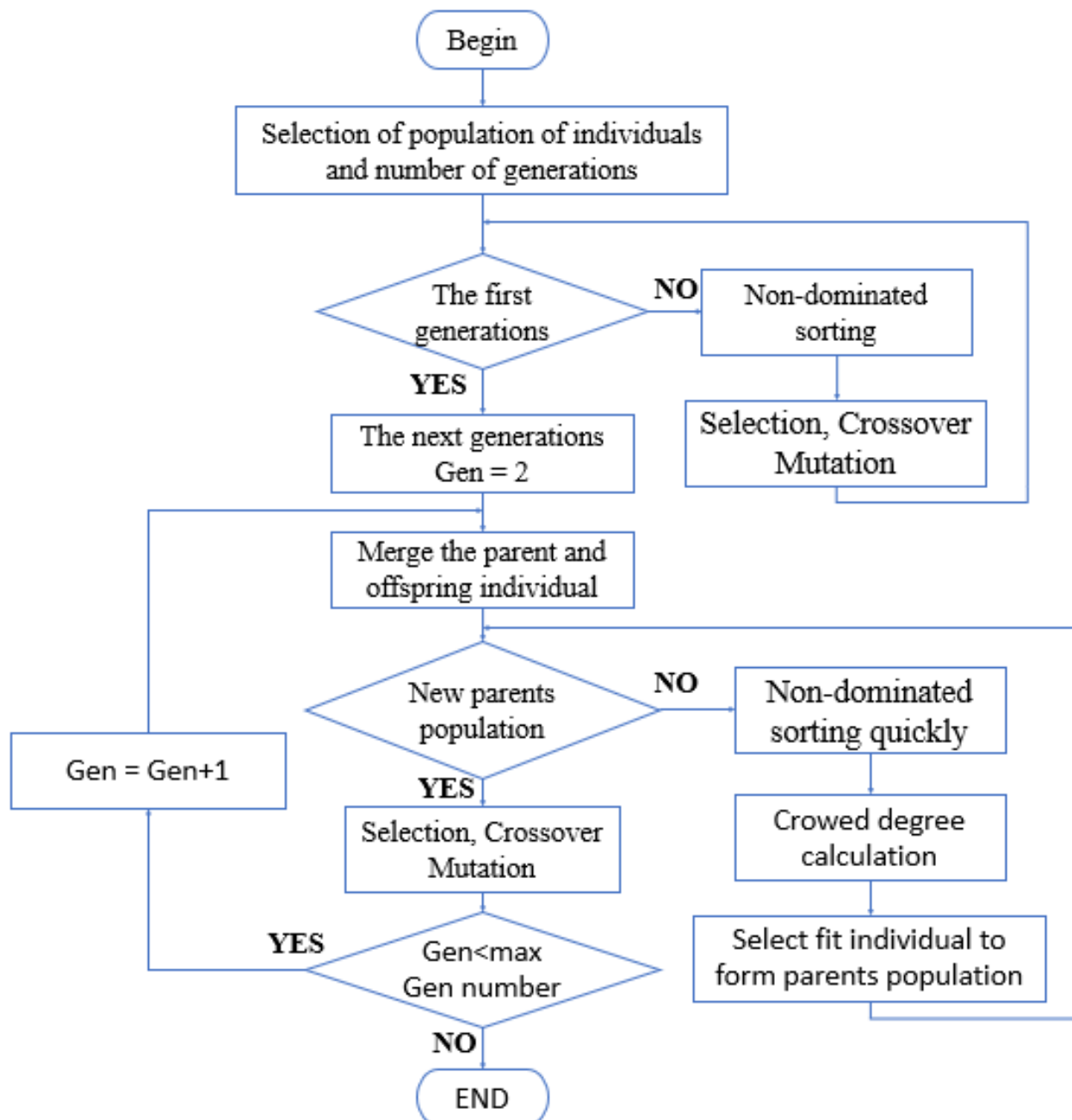

Figure 6. NSGA-II optimization algorithm flow chart.

2.5. MIC Theory

MIC (Maximal Information Coefficient) is the maximum information coefficient. This theory was proposed by Reshef and other scholars in 2011 to measure the degree of correlation between two variables x and y, that is, the strength of linearity or nonlinearity [25]. Compared with Mutual Information (MI, Mutual Information), MIC has higher accuracy

and is an excellent data correlation calculation formula. The calculation formula of MI is shown as:

$$I(x,y) = \int p(x,y) \log_2 \frac{p(x,y)}{p(x)p(y)} dx dy \tag{4}$$

In the formula, $p(x,y)$ is the joint probability between variables x and y; generally, it is difficult to find this value.

The basic principle of MIC is to discretize the relationship between two variables in a two-dimensional space and apply a scatter diagram to represent it [26]. After the current two-dimensional space is divided into a certain number of intervals in the x and y directions, and then check how the current scatter points fall into each grid. This is the calculation of joint probability. This solves the difficult problem of joint probability in mutual information, with the calculation formula below.

$$MIC(x;y) = \max_{a*b<B} \frac{I(x;y)}{\log_2(\min(a,b))} \tag{5}$$

In the formula, a and b are the number of grids divided in the x and y directions, which is essentially the network distribution, and B is a variable, generally taken as the 0.6th power of the amount of data.

3. MLBN Model Development

3.1. Model Construction

Based on the above methods (radio power ratio difference discriminant method, MIC, Stack-LSTM, BAYES, and NSGA-II), this paper proposes a multi-objective optimization-based ensemble probability forecast (MLBN) model. The model couples the integrated modules of data preprocessing, non-stationary period discrimination, feature extraction, deterministic prediction, uncertainty prediction, and optimization, as shown in Figure 7.
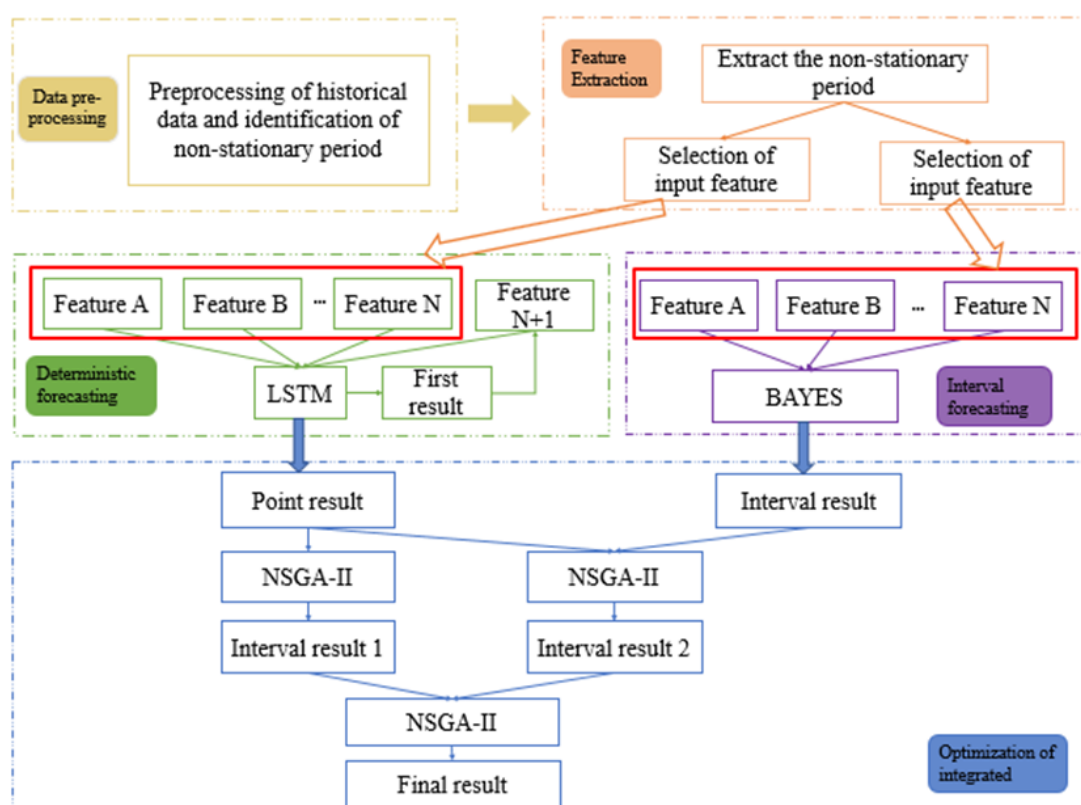

Figure 7. MLBN model framework diagram.

The MLBN proposed in this article is mainly composed of five modules.

Module 1: Data preprocessing and identification of non-stationary periods

(1) Data preprocessing

The central limit theorem (3-Sigma principle) is applied to detect and eliminate abnormal data from the historical output data of photovoltaic power plants, and then adopt the K nearest neighbor algorithm, and the Euclidean distance method to fill in the abnormal data.

(2) Discrimination of non-stationary periods

The pre-processed historical data is discriminated by the method of discriminating the difference in power ratio described above, and two types of periods of steady output and non-stable output are obtained.

Module 2: Feature extraction

Based on the theory of mutual information, this paper chooses the MIC method to extract the input vector features of photovoltaic output data during non-stationary periods, which mainly include the following factors: wind speed, wind direction, temperature, humidity, pressure, and irradiance.

Module 3: Point forecast

The improved Stack-LSTM model algorithm is used to predict the period of photovoltaic non-stationary output with certainty points, and two sets of data from different sources are selected for verification.

Module 4: Interval prediction

The Bayes neural network model is used to predict and verify the interval of uncertainty in the period of photovoltaic non-stationary output.

Module 5: optimize integration forecast

The NSGA-II optimization algorithm is utilized for multi-objective optimization. The prediction results of certainty points and the upper and lower bounds of uncertainty interval prediction are selected as input, and the optimization targets are the largest *PICP* and the smallest *PINAW*.

3.2. Model Prediction Evaluation Index

To evaluate the prediction results of the model more objectively and comprehensively, this paper evaluates the deterministic prediction results from the perspective of certainty, and evaluates the results of interval prediction from the perspective of uncertainty [20].

The deterministic forecast evaluation indicators selected in this paper are the average absolute percentage error (*MAPE*) and root mean square error (*RMSE*). The calculation formula is as follows:

$$MAPE = \frac{1}{N}\sum_{i=1}^{N}\left|\frac{\hat{y}_i - y_i}{y_i}\right| \times 100\% \tag{6}$$

$$RMSE = \sqrt{\frac{1}{N}\sum_{i=1}^{N}\left(\hat{y}_i - y_i\right)^2} \tag{7}$$

In the above formula, N is the number of samples, $\hat{y}_i$ and y_i are the predicted value and actual value at time i, respectively.

Meanwhile, to construct high-quality interval predictions, the indicators used in this paper to evaluate the uncertainty prediction results are the prediction interval coverage probability (*PICP*) and the prediction interval normalized average width (*PINAW*). Interval coverage is the most key indicators to measure wind power prediction effect, reflect the accuracy of forecasting model, the definition refers to the actual wind power value falls within the upper bound and lower bound envelope by the prediction interval of probability, the greater the *PICP*, represent the actual wind power value of the fall in the corresponding prediction interval, interval prediction effect is better, the smaller *PICP* value is, the more actual wind power value is not within the prediction range, and the worse the prediction effect is. The width of the forecast interval can be used to evaluate the quality of the forecast interval from another perspective. In other words, the mean width of the interval (*PINAW*)

is to measure the interval width obtained by the forecast interval. Its mathematical to calculate the mean of all the interval widths over the forecast period.

With the calculation formulas in the following:

$$PICP = \frac{1}{N} \sum_{i=1}^{N} c_i$$
$$c_i = \begin{cases} 1, & \zeta_i \in [L_i, U_i] \\ 0, & \zeta_i \notin [L_i, U_i] \end{cases} \tag{8}$$

where, N is the total number of samples, ζ_i is the actual photovoltaic power, L_i is the lower bound of prediction, and U_i is the upper bound of prediction.

Usually, the performance evaluation index of interval prediction is PICP. If the limit value of the target value is used as the upper and lower boundaries of the prediction interval, 100% PICP can be easily achieved. Too wide the interval leads to an increase in the uncertainty of the forecast results, reduces the instruction of the forecast results for system scheduling, and loses decision-making value. Therefore, it is necessary to quantitatively evaluate the width of the forecast interval [24].

$$PINAW = \frac{1}{NR} \sum_{i=1}^{N} (U_i - L_i) \tag{9}$$

where, R is the variation range of the target value, and using of R can ensure that $PINAW$ is normalized in $[0, 1]$.

4. Results and Discussion

4.1. Data Description

To prove the effectiveness and practicability of the proposed hybrid forecasting model, this paper selects the official data provided by the National Energy Nissin Second Photovoltaic Forecast Competition for forecasting research; the output data of Power Station 1 and Power Station 2 for the whole year of 2017 are selected. The original data is the complete data for the whole year of 2017, and the data time step is 15 min. For the data sampled 24 h a day, there are 32,848 sets of data for power station 1 and 33,060 sets of data for power station 2. Due to the periodicity and intermittent nature of photovoltaic output, this paper only selects the data at the time of daytime power generation. Excluding the data during the non-power generation period at night, and processing and repairing the abnormal data, missing data, and erroneous data in the whole data, finally power station 1 retains a total of 16,018 groups of valid data, and power station 2 retains a total of 16,427 groups of valid data. The first 90% is the training set and the last 10% is the test set. Figure 8 is as follows:
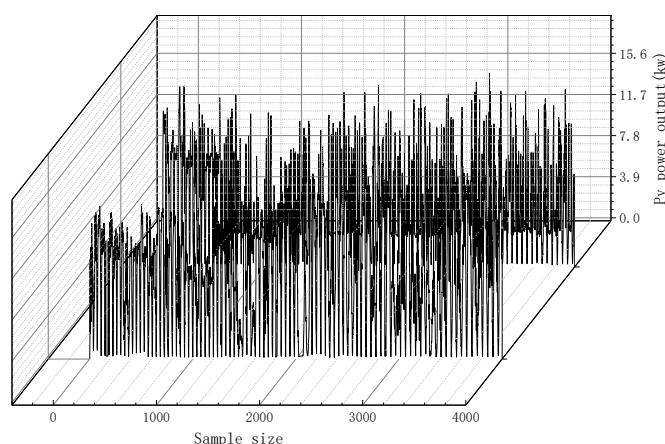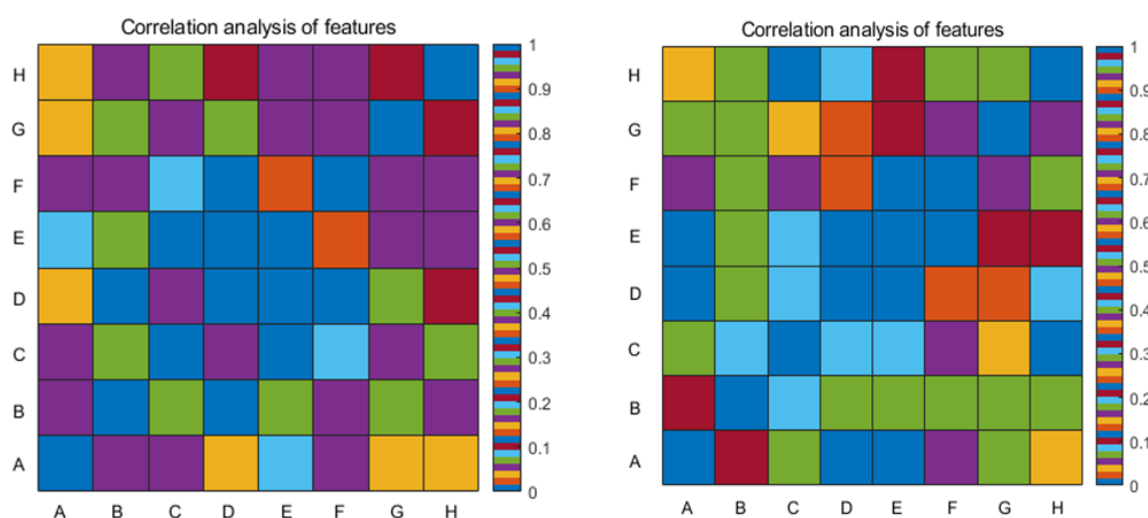

Figure 8. Schematic diagram for data set division.

4.2. Model Input Selection

The purpose of feature selection is to identify a set of optimal feature quantum sets as the input variables of the prediction model. By eliminating irrelevant and redundant variables, the data latitude is reduced, the amount of calculation is reduced, and the training process of the model is accelerated. Appropriate feature selection is one of the key factors to improve the performance of prediction models based on machine learning algorithms [30]. The data of each sample in the data set used in this article includes 1-dimensional historical photovoltaic power generation and 6-dimensional influencing factor variables, as detailed in Table 1. The results obtained by MIC theory analysis are shown in Figure 9.

Table 1. Data composition of sample points.

Number	Variate	Whether
1	The actual output value of photovoltaic power station	
2	Wind speed	√
3	Wind direction	√
4	Temperature	√
5	Humidity	√
6	Intensity	
7	Irradiance	√

A: Irradiance　B: Wind speed　C:Wind direction　D: Temperature　E: Humidity　F:Intensity　G: Solar power　H: Power

Figure 9. Selection table of characteristic factors.

It can be obtained from the MIC result graph that in the two sets of data, the factors with strong nonlinear correlation include irradiance, humidity, temperature, and wind speed, so these factors are selected as the model inputs of this paper.

4.3. Point Prediction Result

According to the above-mentioned results from MIC, the input variables are selected for the Stack-LSTM model. The data 1 and data 2 are validated by the evaluation indexes (*MAPE, RMSE*) for this model to get its prediction curve, respectively shown in Figure 10a,b. To use these two sets of results as a control group, LSTM and ANN models are selected as the benchmark model, as shown in Figure 10c–f.
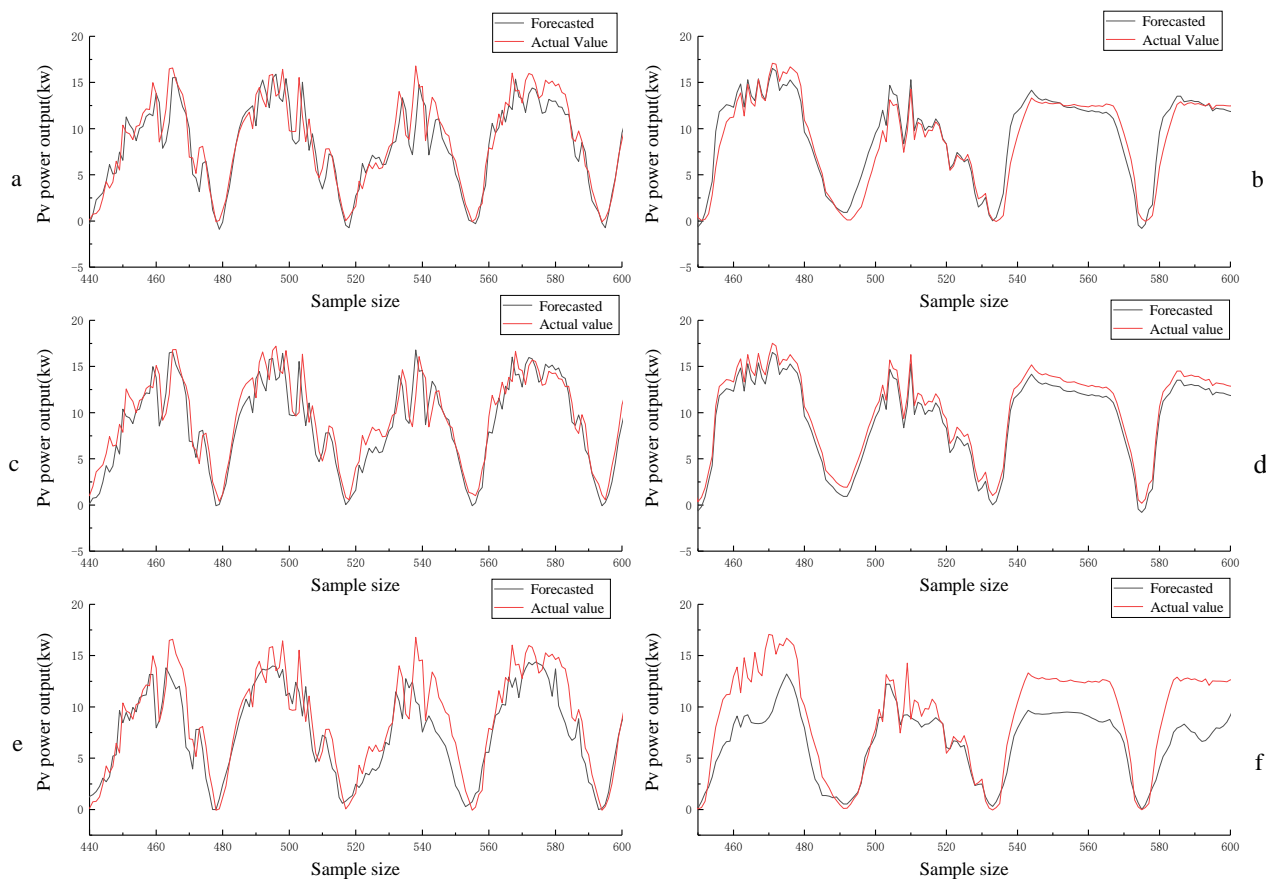
Figure 10. Multiple point prediction model diagram.

From Figure 11, compared with the original LSTM model and ANN model, the Stack-LSTM model has the highest curve fit and prediction accuracy through the improvement of the non-stationary photovoltaic output period prediction model. To accurately quantify the improvement of prediction accuracy, Table 2 provides a comparison of indicators for evaluating the prediction effect of the model.

Table 2. Comparison of multi-model MAPE.

Number	Text	ANN (%)	LSTM (%)	Stack-LSTM (%)	Rate of Rise
	1	1.10306	0.72771	0.50218	0.22553
	2	1.12407	0.73006	0.49782	0.23224
Station 1	3	1.08590	0.72827	0.50116	0.22711
	4	1.12504	0.72735	0.49835	0.21900
	1	0.95952	0.70039	0.51487	0.18552
	2	0.95643	0.71264	0.51035	0.20229
Station 2	3	0.96076	0.70982	0.50273	0.20709
	4	0.94895	0.69331	0.51640	0.17691

According Table 2, through the improvement of the prediction model for the non-stationary photovoltaic output period, the prediction accuracy of the Stack-LSTM model is compared with the original LSTM model and the traditional ANN network, and the accuracy is improved by nearly 20% and 30%, which verify the feasibility and practicability of the Stack-LSTM model.
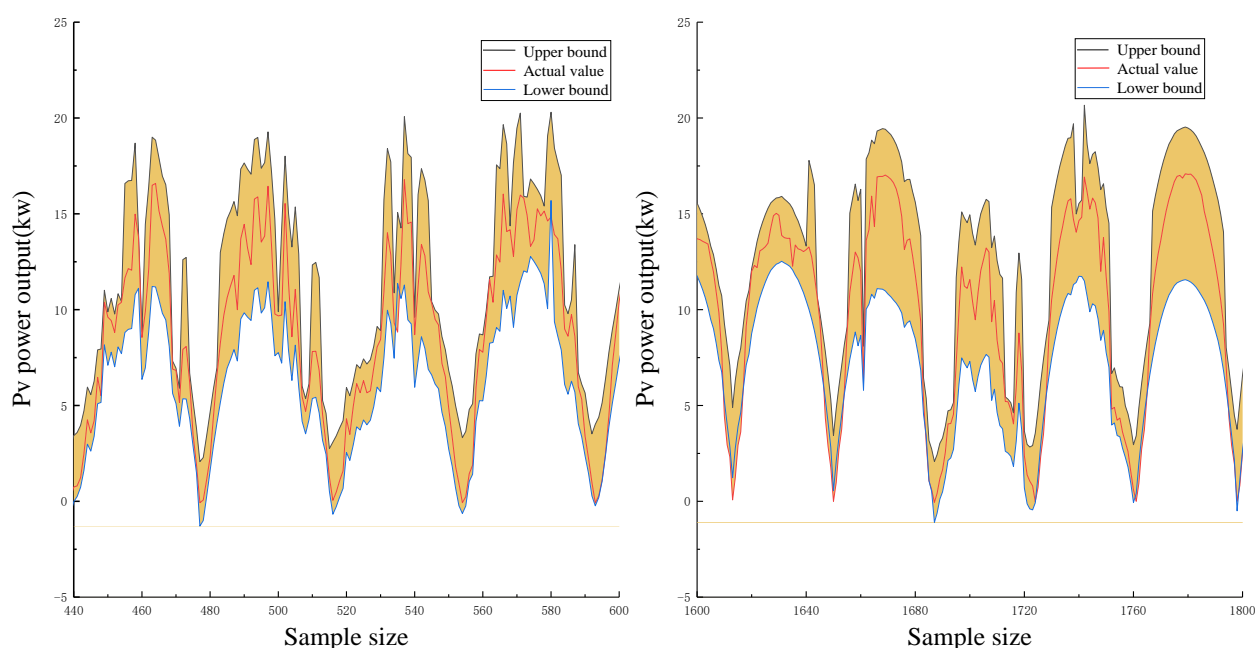
Figure 11. Interval prediction model diagram.

4.4. Interval Prediction Result

Through the MIC analysis results, the input features are selected, and the BAYES neural network prediction of the two sets of data is performed, with the prediction results shown in Figure 11. The relative interval widths under the coverage rates of 85%, 90%, and 95% are calculated respectively, as shown in Table 3.

Table 3. Comparison before and after multi-objective optimization

Number	PICP	Reference [18]	Before PINAW	After PINAW	Rate of Rise (%)
	85%	9.0342	7.4852	6.2607	17.56
Station 1	90%	9.4976	7.7087	6.8395	12.84
	95%	10.1306	8.2711	7.7403	10.41
	85%	9.0342	7.2975	6.4453	13.38
Station 2	90%	9.4976	7.6542	7.0842	9.86
	95%	10.1306	7.9583	7.2574	9.65

It can be seen from the Figure 12, that compared with deterministic point prediction, using the Bayesian neural network for interval prediction has a better ability to suppress the risk of overfitting than ordinary neural networks. During the non-steady output period, it can predict the possible output at that point, so that the dispatching system can adjust the dispatching strategy in time to ensure the safe and stable operation of the power grid to the greatest extent.

4.5. Optimization of Ensemble Prediction Results

In order to improve the overall prediction accuracy, select the prediction results of certain points and the upper and lower bounds of the uncertainty interval prediction as input. The optimization targets are the largest *PICP* and the smallest *PINAW*. The NSGA-II optimization algorithm is used for multi-objective optimization, Figure 12 shows the comparison of its prediction interval results.
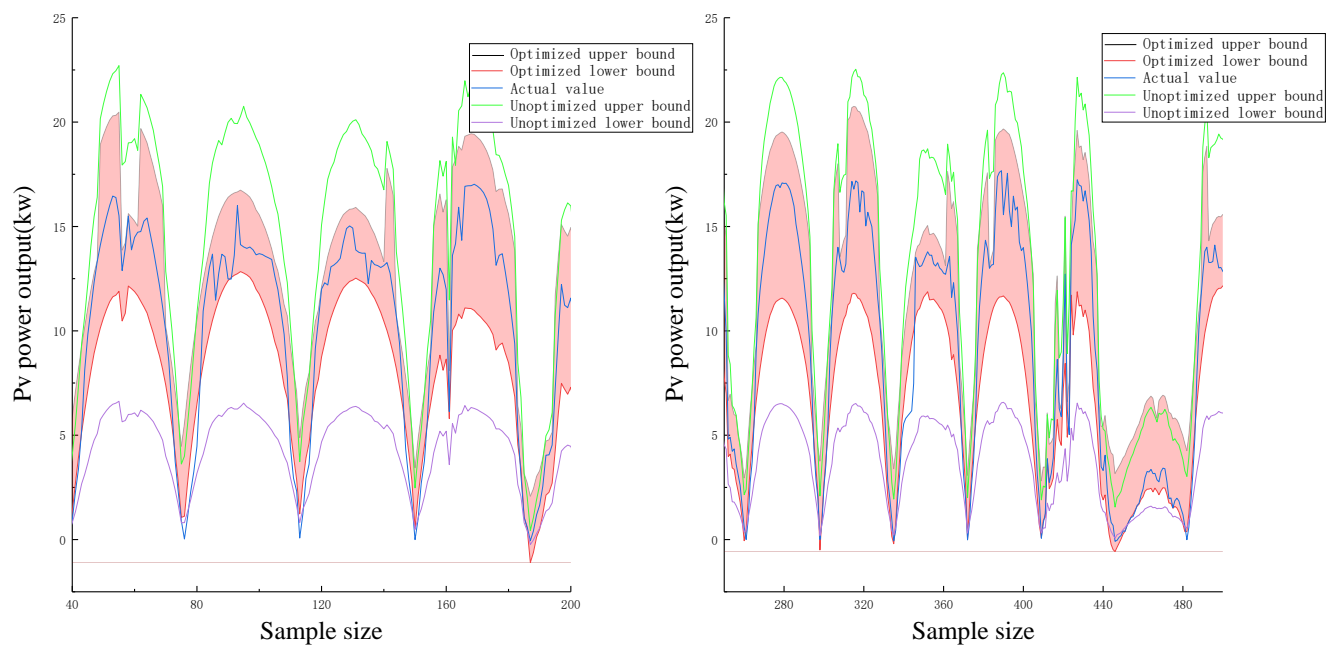
Figure 12. Comparison of power stations 1 and 2.

The shaded part in the Figure 12 is the interval boundary value optimized by this article. The green and purple straight lines represent the unoptimized, original interval prediction upper and lower boundary values. On the premise of ensuring interval coverage, after the optimization processing in this article, the interval width has been greatly narrowed and the prediction accuracy has been greatly improved under the premise of ensuring the coverage of the interval. To quantify the degree of increase in this uncertainty, specific data pairs are shown in Table 3.

From Table 3, under the same interval coverage, the prediction model compared with the unoptimized prediction model is obtained. The width of the interval in this article has been reduced by 10–20%, which means that the prediction accuracy has increased by at least 10%. Compared with the boundary estimation theory method described in reference [18], under the same interval coverage, the MLBN prediction model constructed in this paper performs multi-objective optimization on the deterministic prediction results and the interval prediction results, and the prediction accuracy is improved by more than 20%, which proves the feasibility of constructing the model in this paper. The accuracy improvement shown by the experimental data enables the dispatching system to more accurately evaluate the fluctuation of photovoltaic output based on the width of the interval, which is of great significance to the safe and stable operation of the power grid.

5. Conclusions

Aiming at the problem of poor prediction accuracy of traditional photovoltaic power prediction models during non-stationary periods of photovoltaic output, this paper proposes an ensemble probability prediction (MLBN) model based on multi-objective optimization, the conclusions are as the follows:

(1) The model combines with data preprocessing, non-stationary period discrimination, feature extraction, deterministic prediction, uncertainty prediction, and optimization integration modules to construct a difference in power ratio discrimination method and a Stack-LSTM point prediction model. The proposed MLBN model combines mainstream deterministic forecasting models and interval forecasting models, fusing point forecasting and interval forecasting, and performing multi-objective optimization on two different forms of forecasting results.

(2) After improving the prediction in this article, the prediction accuracy of the Stack-LSTM model is 20% higher than that of the original LSTM model, and compared with the traditional ANN network, the accuracy is improved by nearly 30%, verifying the feasibility and practicality of the model constructed in this article.

(3) Under the PICP of 85%, 90% and 95%, the interval forecast can predict the possible output of this point as far as possible in the non-stationary output period, which enables the dispatching system to timely adjust the dispatching strategy and ensure the safe and stable operation of the power grid to the greatest extent.

(4) Compared with the unoptimized prediction model, the interval width is reduced by 10–20% and the prediction accuracy is improved by at least 10% under the uniform interval coverage, which significantly improves the prediction accuracy of photovoltaic power prediction and verifies the feasibility of the proposed method.

The novelty of the work relies on combining point prediction and interval prediction, focusing on interval prediction. The results show that the MLBN model can significantly improve the prediction accuracy of photovoltaic power prediction, which can greatly facilitate grid planning, risk analysis and reliability evaluation. At the same time, accurate photovoltaic power forecast can carry out effective scheduling and scientific management of photovoltaic power stations, improve the ability of power grid to accept photoelectricity, guide the deficiency elimination and planned maintenance of photovoltaic power stations, and improve the operation economy of photovoltaic power stations. And this model has great benefits to promote the efficient planning of renewable energy system operations and smart grid systems in obtaining multiple energy sources.

In the further research, this article will try as follows. One is to well combine the deterministic prediction and uncertainty prediction models since this article to further increase the prediction accuracy; the second is to try to higher-level machine learning methods to study the prediction of photovoltaic power interval in the whole climate field, increase the prediction duration, and improve the prediction accuracy.

Institutional Review Board Statement: Not applicable.

Informed Consent Statement: Not applicable.

Data Availability Statement: Not applicable.

Conflicts of Interest: The authors declare no conflict of interest.

Abbreviations

PV	Photovoltaic
LSTM	long-short-term memory neural network
Stack-LSTM	Stacking- long-short-term memory neural network
LSTM-RNN	long-short-term recurrent neural network
ELM	extreme learning machine
LUBE	lower and upper bound estimation
DM	Discrimination method for radiation power ratio difference
NSGA-II	Non-dominated Sorting Genetic Algorithm-II

MIC	Maximal Information Coefficient
RNN	recurrent neural network
MI	Mutual Information
MAPE	average absolute percentage error
RMSE	root mean square error
PICP	prediction interval coverage probability
PINAW	prediction interval normalized average width

References

1. Li, P.; Zhou, K.; Lu, X.; Yang, S. A hybrid deep learning model for short-term PV power forecasting. *Appl. Energy* **2020**, *259*, 114216. [CrossRef]
2. Jung, Y.; Jung, J.; Kim, B.; Han, S. Long short-term memory recurrent neural network for modeling temporal patterns in long-term power forecasting for solar PV facilities: Case study of South Korea. *J. Clean. Prod.* **2020**, *250*, 119476. [CrossRef]
3. Teng, X.; Gao, Z.; Zhang, Y.; Huang, H.; Li, L.; Liang, T. Key technologies and the implementation of wind, PV and storage co-generation monitoring system. *J. Mod. Power Syst. Clean Energy* **2014**, *2*, 104–113. [CrossRef]
4. Ni, Q.; Zhuang, S.; Sheng, H.; Kang, G.; Xiao, J. An ensemble prediction intervals approach for short-term PV power forecasting. *Sol. Energy* **2017**, *155*, 1072–1083. [CrossRef]
5. Ahmed, R.; Sreeram, V.; Mishra, Y.; Arif, M. A review and evaluation of the state-of-the-art in PV solar power forecasting: Techniques and optimization. *Renew. Sustain. Energy Rev.* **2020**, *124*, 109792. [CrossRef]
6. Chu, Y.; Coimbra, C.F. Short-term probabilistic forecasts for Direct Normal Irradiance. *Renew. Energy* **2017**, *101*, 526–536. [CrossRef]
7. Rahimi, M.; Ardakani, F.J.; Ardakani, A.J. Optimal stochastic scheduling of electrical and thermal renewable and non-renewable resources in virtual power plant. *Int. J. Electr. Power Energy Syst.* **2021**, *127*, 106658. [CrossRef]
8. Chen, H.H.; Wang, Y.; Zhang, R.F.; Guo, F.; Jia, M.; Sun, D.F. Spinning reserve capacity optimization considering coordination between source and load or power system with wind power. *Electr. Power Autom.* **2017**, *38*, 185–192. [CrossRef]
9. Guo, W.; Liu, P.; Shu, X. Optimal dispatching of electric-thermal interconnected virtual power plant considering market trading mechanism. *J. Clean. Prod.* **2021**, *279*. [CrossRef]
10. Sakr, W.S.; El-Ghany, H.A.A.; El-Sehiemy, R.A.; Azmy, A.M. Techno-economic assessment of consumers' participation in the demand response program for optimal day-ahead scheduling of virtual power plants. *Alex. Eng. J.* **2020**, *59*, 399–415. [CrossRef]
11. Lee, D.; Kim, K. PV power prediction in a peak zone using recurrent neural networks in the absence of future meteorological information. *Renew. Energy* **2020**, *1*. [CrossRef]
12. Xiao, C.; Sutanto, D.; Muttaqi, K.M.; Zhang, M. Multi-period data driven control strategy for real-time management of energy storages in virtual power plants integrated with power grid. *Int. J. Electr. Power Energy Syst.* **2020**, *118*. [CrossRef]
13. Vandeventer, W.; Jamei, E.; Thirunavukkarasu, G.S.; Seyedmahmoudian, M.; Soon, T.K.; Horan, B.; Mekhilef, S.; Stojcevski, A. Short-term PV power forecasting using hybrid GASVM technique. *Renew. Energy* **2019**, *140*, 367–379. [CrossRef]
14. Oneto, L.; Laureri, F.; Robba, M.; Delfino, F.; Anguita, D. Data-driven photovoltaic power production nowcasting and forecasting for polygeneration microgrids. *IEEE Syst. J.* **2018**, *12*, 2842–2853. [CrossRef]
15. El-Baz, W.; Tzscheutschler, P.; Wagner, U. Day-ahead probabilistic PV generation forecast for buildings energy management systems. *Sol. Energy* **2018**, *171*, 478–490. [CrossRef]
16. Gao, M.; Li, J.; Hong, F.; Long, D. Day-ahead power forecasting in a large-scale photovoltaic plant based on weather classification using LSTM. *Energy* **2019**, *187*, 115838. [CrossRef]
17. Yang, X.; Xu, M.; Xu, S.; Han, X. Day-ahead forecasting of photovoltaic output power with similar cloud space fusion based on incomplete historical data mining. *Appl. Energy* **2017**, *206*, 683–696. [CrossRef]
18. Wang, F.; Xuan, Z.; Zhen, Z.; Li, K.; Wang, T.; Shi, M. A day-ahead PV power forecasting method based on LSTM-RNN model and time correlation modification under partial daily pattern prediction framework. *Energy Convers. Manag.* **2020**, *212*, 112766. [CrossRef]
19. Li, K.; Wang, R.; Lei, H.; Zhang, T.; Liu, Y.; Zheng, X. Interval prediction of solar power using an Improved Bootstrap method. *Sol. Energy* **2018**, *159*, 97–112. [CrossRef]
20. Zhang, X.; Wang, R.; Liao, T.; Zhang, T.; Zha, Y. Short-Term Forecasting of Wind Power Generation Based on the Similar Day and Elman Neural Network. In Proceedings of the 2015 IEEE Symposium Series on Computational Intelligence, Cape Town, South Africa, 7–10 December 2015; pp. 647–650.
21. Raza, M.Q.; Mithulananthan, N.; Summerfield, A. Solar output power forecast using an ensemble framework with neural predictors and Bayesian adaptive combination. *Sol. Energy* **2018**, *166*, 226–241. [CrossRef]
22. Bouzerdoum, M.; Mellit, A.; Pavan, A.M. A hybrid model (SARIMA–SVM) for short-term power forecasting of a small-scale grid-connected photovoltaic plant. *Sol. Energy* **2013**, *98*, 226–235. [CrossRef]
23. Tan, Q.; Mei, S.; Dai, M.; Zhou, L.; Wei, Y.; Ju, L. A multi-objective optimization dispatching and adaptability analysis model for wind-PV-thermal-coordinated operations considering comprehensive forecasting error distribution. *J. Clean. Prod.* **2020**, *256*, 120407. [CrossRef]
24. Kushwaha, V.; Pindoriya, N.M. A SARIMA-RVFL hybrid model assisted by wavelet decomposition for very short-term solar PV power generation forecast. *Renew. Energy* **2019**, *140*, 124–139. [CrossRef]

25. Hao, Y.; Dong, L.; Liang, J.; Liao, X.; Wang, L.; Shi, L. Power forecasting-based coordination dispatch of PV power generation and electric vehicles charging in microgrid. *Renew. Energy* **2020**, *155*, 1191–1210. [CrossRef]

26. Almeida, M.P.; Muñoz, M.; De La Parra, I.; David, M. Comparative study of PV power forecast using parametric and nonparametric PV models. *Sol. Energy* **2017**, *155*, 854–866. [CrossRef]

27. Oprea, S.-V.; Bâra, A. Ultra-short-term forecasting for photovoltaic power plants and real-time key performance indicators analysis with big data solutions. Two case studies-PV Agigea and PV Giurgiu located in Romania. *Comput. Ind.* **2020**, *120*. [CrossRef]

28. Das, S. Short term forecasting of solar radiation and power output of 89.6 kWp solar PV power plant. *Mater. Today Proc.* **2020**. [CrossRef]

29. LaBar, H.; Samira, K.M. Optimal PV panel's end-life assessment based on the supervision of their own aging evolution and waste management forecasting. *Sol. Energy* **2019**, *191*, 227–234. [CrossRef]

30. Angenendt, G.; Zurmühlen, S.; Axelsen, H.; Sauer, D.U. Comparison of different operation strategies for PV battery home storage systems including forecast-based operation strategies. *Appl. Energy* **2018**, *229*, 884–899. [CrossRef]